# VIBRATION ATTENUATION IN A SEMI-PASSIVE FRAME BASED ON REINFORCEMENT LEARNING ALGORITHM

# GRZEGORZ MIKUŁOWSKI, DOMINIK PISARSKI, BŁAŻEJ POPŁAWSKI AND ŁUKASZ JANKOWSKI

Institute of Fundamental Technological Research
Polish Academy of Sciences
ul. Pawińskiego 5b, 02-106 Warsaw, Poland
e-mail: gmikulow@ippt.pan.pl, web page: http://www.ippt.pan.pl/

**Abstract.** This contribution addresses the problem of adaptively tuning the parameters of semi-active devices to mitigate vibrations in structures subjected to unknown periodic excitation. Using a specially designed reinforcement learning algorithm, the semi-active devices adjust their operating parameters to ensure optimal dissipation of vibrational energy. The algorithm incorporates an efficient gradient-based sequence that ensures rapid convergence of the learning process and enables real-time implementation under varying excitation characteristics. The method is experimentally validated on a frame structure equipped with lockable joints, which can be controlled to adjust their stiffness parameters. Since the developed reinforcement learning algorithm incorporates partial knowledge of the structural model, the first part of the work is focused on formulating a simplified numerical model that is easy to identify and scale.

**Key words:** Vibration attenuation, Reinforcement Learning, Semi-active control, Adaptive structure, Stiffness control

#### 1 INTRODUCTION

Vibrations of engineering structures result from operational or external excitation. Excessive vibration levels endanger integrity and jeopardize the operation of structures and machines. This problem is further exacerbated by the current trend toward cost-effective and lightweight structural design. Mitigation of vibrations is thus the subject of intensive research and development activities [1]. Typical techniques can be categorized into passive, active, and semi-active control approaches. Passive techniques usually employ dedicated dissipative elements and/or rely on structural optimization. A classical passive device is the tuned mass damper (TMD). Low cost, reliability, and design simplicity are the main advantages of these techniques; however, their efficiency is limited in many situations. Active control approaches are effective and widely researched [2], but they rely on actuators that generate large control forces and require significant power supply, which may fail during events such as major earthquakes. Moreover, in the case of a control system malfunction, large control forces can lead to structural instability.

Semi-active control techniques often combine the advantages of passive and active systems. Instead of generating large external control forces, semi-active actuators modify structural dynamics [3] by affecting local mechanical parameters such as damping, stiffness, or kinematic constraints [4]. They are typically implemented using magnetorheological fluids (in mid-to large-scale applications) or piezoelectric materials (for small-scale control) and may take the form of frictional joints [5] or switched oil dampers [6]. They can be implemented with limited power supply and in a fail-safe manner, while often similarly efficient as active systems. However, the control functions are coupled to the local structural response. The corresponding formulations are thus nonlinear and difficult to solve using classical analytical approaches.

Reinforcement learning (RL) has achieved significant breakthroughs in autonomous control and decision-making, with demonstrated success across a variety of real-world applications, from mastering complex games like chess and Go at superhuman levels [7] to thermal soaring of autonomous gliders [8], robotic swimming via body undulation [9], and self-driving vehicles [10]. Despite RL's success and algorithmic adaptability, its application to structural vibration problems remains limited. Most existing studies focus on active control approaches, often implemented in structures with only a few degrees of freedom. In [11], a deep deterministic policy gradient RL algorithm (DDPG) was used to control a simulated, partially observable six degree of freedom (DOF) shear structure equipped with a force actuator on the first floor. In [12], DDPG was employed to train neural networks for controlling a flexible hinged plate with piezoelectric actuators. Experimental results confirmed that the RL-based control strategy achieved superior stability performance compared to conventional proportional-derivative (PD) control. In [13], the Q-learning RL technique was applied to optimize fuzzy-PD controller parameters for vibration suppression in high-rise buildings. The method was validated under diverse seismic conditions and demonstrated robustness against control loop time delays. In [14], the authors implemented an actor-critic RL algorithm to stabilize a swinging chain at a target position. Their active control approach operated with incomplete state information. While outperformed by model-based analytic solutions, this method presents a viable alternative for scenarios where accurate system modeling is not possible. The application of RL for shape control in active tensegrity structures was suggested in [15]. The algorithm integrated casebased reasoning with error-driven learning, demonstrating both enhanced control precision and reduced computational burden compared to conventional methods. An RL-based algorithm to stabilize free vibrations in semi-active, simply supported beams was developed in [16]. The proposed method optimizes switching controller parameters to adapt to changing excitation force characteristics. A deep Q-network approach (DQN) was used in [17] to mitigate seismic vibrations in a simulated 11-DOF shear structure equipped with an on/off-type semi-active tuned mass damper (TMD). The RL-based control reduced the RMS of the top floor displacements to 75% of that achieved with the same TMD optimally tuned but passive. The same structure was used in [18] to evaluate and confirm the high robustness of the DQN-based semi-active control to model errors and measurement noise. In [19], the neural network of the RL agent was extended to a two-branch configuration with shared features. This architecture enabled simultaneous identification of stiffness-related damage along with semi-active control.

This paper develops an actor-only reinforcement learning algorithm for optimizing the parameters of semi-active actuators installed on a vibrating structure subjected to unknown periodic excitation. First, the control and learning techniques are presented. Then, their performance is verified using a lab-scale frame structure equipped with six semi-active joints that control the effective stiffness of the structure.

### 2 RL-DRIVEN ACTUATOR PARAMETER ADJUSTMENT

This work studies a class of semi-passive vibrating structures that can be characterized by the ordinary bilinear differential equation:

$$\dot{x}(t) = A x(t) + \sum_{i=1}^{m} u_i(t) B_i x(t) + F(t), \qquad x(0) = x^0.$$
 (1)

In Eq. (1), the state vector at time t is given by  $x(t) = [x_1(t), ..., x_n(t)]^T \in \mathbb{R}^n$ , with an initial condition  $x^0$ . The parameters  $u_1(t), ..., u_m(t)$ , where  $u_i(t) \in \mathcal{U} \subset \mathbb{R}_+$ , are assumed to be piecewise constant and determine the tunable stiffness/damping of the incorporated actuators. The constant matrices A and  $B_1, ..., B_m$ , each of size  $n \times n$ , represent the internal subsystem dynamics and the influence of the ith semi-active device, respectively. The excitation force F(t), an  $n \times 1$  vector, is assumed to be periodic but unknown.

The aim is to develop a Reinforcement Learning algorithm that tunes the control policy P defined as fixed actuator parameters:

$$P: \{u_1, ..., u_m\} \tag{2}$$

to unknown characteristics of the excitation force F(t). The algorithm employs an actor-only framework (Figure 1), utilizing state measurements x(t) over a learning time window T. The algorithm iteratively reduces the value of the following energy-related performance measure:

$$J = \int_{t_0}^{t_0 + T} x^{\mathsf{T}}(t) \, Q \, x(t) \, \mathrm{d}t. \tag{3}$$

$$Policy \, parameters \\ u_1, \dots, u_m \qquad \qquad Environment \\ \dot{x} = f(x, u_1, \dots, u_m, F) \qquad Unknown \, \text{excitation} \, (F)$$

$$(\Delta u_1, \dots, \Delta u_m) \qquad Policy \, \text{gradient} \\ \frac{\delta J}{\delta u_1}, \dots, \frac{\delta J}{\delta u_m}$$

Figure 1: Schematic of Reinforcement Learning-driven actuator parameters (policy parameters) adjustment to unknown excitation forces. The actor's policy is iteratively optimized through interaction with the dynamical system environment. The policy gradients used for updating the policy parameters employ the real-time measurements of system state x and adjoint state y computed by backward integration of the adjoint dynamics (Eq. (6)).

Here,  $t_0$  is a time instant that will be incremented during the adjustment process, while the time window T is selected to be sufficiently large to ensure the decay of transient vibrations, given the assumption of a periodic excitation force F (consistent reduction of the performance measure requires steady-state vibration conditions). The  $n \times n$  matrix Q is constant and positive definite. The adjustment of the policy parameters  $u_1, ..., u_m$  is based on the gradient descent method:

$$u_i^+ = u_i - \alpha_i \frac{\delta J}{\delta u_i}, \quad i = 1, ..., m, \quad \alpha > 0.$$
 (4)

To compute the derivatives in Eq. (4), we introduce the Hamiltonian H for objective functional defined by Eq. (3) and the dynamical system Eq. (1), assuming that  $u_1, ..., u_m$  are constant for  $t \in [t_0, t_0 + T]$ :

$$H(x, p, \{u_i\}_{i=1,\dots,m}) = p^{\mathsf{T}} \left( A x + \sum_{i=1}^{m} u_i B_i x + F \right) - \frac{1}{2} x^{\mathsf{T}} Q x.$$
 (5)

The adjoint state  $p(t) = [p_1(t), ..., p_n(t)]^T \in \mathbb{R}^n$  satisfies the following differential equation:

$$\dot{p}(t) = -\frac{\partial H}{\partial x} = -A^{\mathrm{T}} p(t) - \sum_{i=1}^{m} u_i B_i^{\mathrm{T}} p(t) + Qx(t), \qquad p(t_0 + T) = 0.$$
 (6)

From Eq. (1) and Eq. (5), the objective functional Eq. (3) can be represented by:

$$J = \int_{t_0}^{t_0+T} \left( p^{\mathsf{T}} \dot{x} - H(x, p, \{u_i\}_{i=1,\dots,m}) \right) dt.$$
 (7)

Let the functions  $\delta x: [t_0, t_0 + T] \to R^n$  and  $\delta p: [t_0, t_0 + T] \to R^n$  denote perturbations of the functions x and p with respect to the infinitesimal changes  $\mathrm{d} u_i: R \to R, i=1,...,m$  of  $u_i$ , respectively. From Eq. (7), it follows that the differential  $\delta J$  of the objective functional Eq. (3) with respect to perturbations  $\delta u_i, i=1,...,m$  is given by:

$$\delta J = \int_{t_0}^{t_0+T} \left( -\sum_{i=1}^m \frac{\partial H}{\partial u_i} \delta u_i - \left( \frac{\partial H}{\partial x} \right)^{\mathrm{T}} \delta x \right) \mathrm{d}t + \int_{t_0}^{t_0+T} \left( p^{\mathrm{T}} \delta \dot{x} + \left( \dot{x} - \frac{\partial H}{\partial p} \right)^{\mathrm{T}} \delta p \right) \mathrm{d}t.$$
 (8)

The last term in Eq. (8) vanishes, since

$$\dot{x} = \frac{\partial H(x, p, \{u_i\}_{i=1,\dots,m})}{\partial p}.$$
(9)

From the differentiability of the state vector x with respect to t, it follows that:

$$\delta \dot{x} = \frac{\mathrm{d}}{\mathrm{d}t} \left( \delta x \right). \tag{10}$$

Using the assumption given by Eq. (10), we can perform the integration by parts for Eq. (8), which results in

$$\delta J = -\int_{t_0}^{t_0+T} \sum_{i=1}^m \frac{\partial H}{\partial u_i} \, \delta u_i \, \mathrm{d}t - \int_{t_0}^{t_0+T} \left( \dot{p} + \frac{\partial H}{\partial x} \right)^{\mathrm{T}} \delta x \, \mathrm{d}t + \left[ p^{\mathrm{T}} \delta x \right]_{t_0}^{t_0+T}. \tag{11}$$

From Eq. (1) and Eq. (6), it can be deduced that

$$\dot{p} = -\frac{\partial H}{\partial x}, \qquad p(t_0 + T) = 0, \qquad \delta x(t) = 0,$$
 (12)

and therefore, the second and the last term in Eq. (11) vanish. As a result, the derivative of the objective functional J with respect to  $u_i$  is given by:

$$\frac{\delta J}{\delta u_i} = -\int_{t_0}^{t_0+T} p^{\mathrm{T}} B_i x \, \mathrm{d}t. \tag{13}$$

To compute the derivatives in Eq. (13), the online algorithm will use the state x, measured by integrated sensors, and the adjoint state p, obtained through backward integration of Eq. (6). Note that the adjoint state dynamical equation does not explicitly depend on the external excitation force F. Instead, the influence of F is embedded in the measured state x. Thus, the adjustment of the policy parameters  $u_1, ..., u_m$  is achieved through interaction with the dynamical system, reflecting the core assumption of reinforcement learning techniques.

### 3 EXPERIMENTAL VERIFICATION

The proposed control approach is verified on a small-scale demonstrator in laboratory conditions. The demonstrator is a cantilever frame structure equipped with 6 semi-active joints, configured in 3 pairs. These joints allow for modification of the local stiffness of the structure by locking and unlocking their angular degrees, which enables control of the bending moments transferred between adjacent components of the structure. The experimental scenario involves forced excitation of the structure with an unknown, varying input. The bandwidth of the harmonic excitation includes the resonant frequency. Compared to the passive case, the results demonstrate that the algorithm efficiently adapts the structural response to the unknown varying excitation and reduces the energy level of the structural response.

### 4 EXPERIMENTAL DEMONSTRATOR

The experimental object is a cantilever frame subjected to external excitation by an electrodynamic shaker (see Figure 2). The frame consists of two parallel longitudinal segments, each 1.2 m long, connected by transverse beams. It is equipped with six semi-active joints that connect the longitudinal and transverse segments. The joints ensure a passive transfer of planar bending moments between the longitudinal components while enabling controlled moment transfer to the transverse segments. The semi-active elements are organized in 3 pairs, mounted at equal distances of 0.3 m, starting 0.6 m from the fixed end of the frame. Each pair is activated simultaneously, which allows for local modification of structural stiffness.

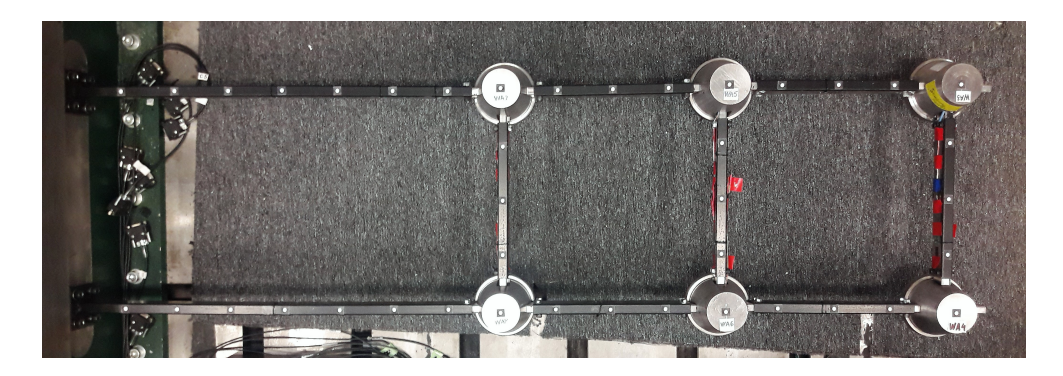


Figure 2: Experimental frame with 3 pairs of semi-actively controlled joints

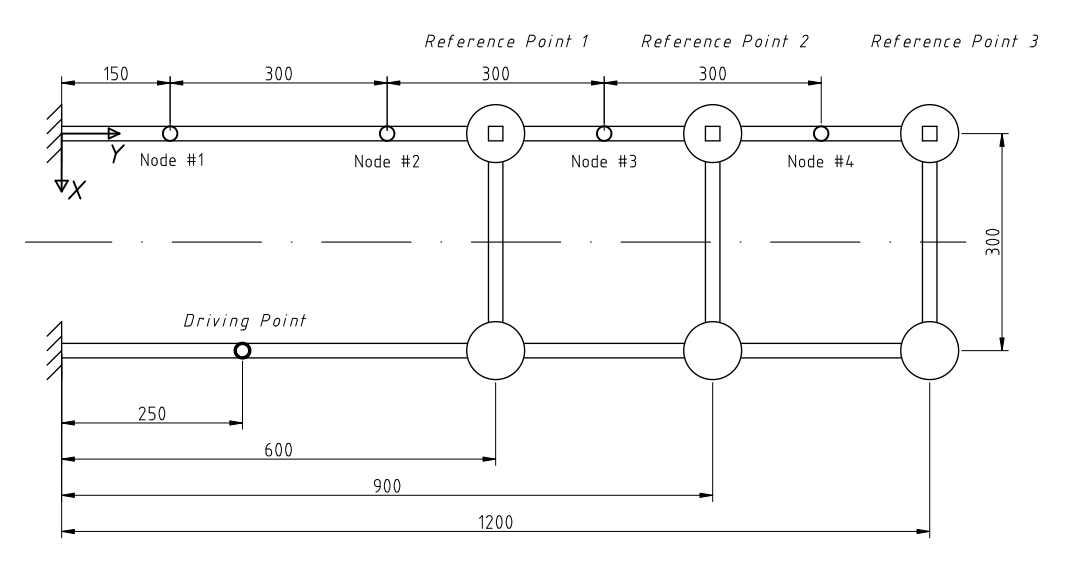


Figure 3: Scheme of the experimental frame setup

# 4.1 Assumptions

A planar coordinate system is adopted for kinematic analysis of the frame. This choice is determined by the design of the actuators, which implement structural modifications exclusively within the plane of the structure. The OXY coordinate system is shown in Figure 3.

Another assumption is that the demonstration frame structure can be accurately modeled with a 1D Timoshenko beam model. The frame design and its semi-active components emphasize the importance of both bending and shear stress control. The adopted numerical model, based on the Timoshenko beam, accounts for shear effects and their intentional modification. The validity of this assumption is experimentally confirmed by spectral analysis and model validation.

The data acquisition and excitation systems are configured in accordance with the above assumptions. The system is analyzed in-plane, with sensors and the exciter arranged to acquire data in the OXY plane. Displacements are measured for one longitudinal segment of the frame, based on the assumption that the response of the other segment is symmetrical.

#### 4.2 Excitation

The frame is operated under forced vibration conditions. The source of vibrations is a modal shaker connected in the Driving Point and providing excitation in the OX direction, as depicted in Figure 3. The excitation signal depends on the particular task being carried out. First, a downward frequency sweep from 16 Hz down to 6 Hz was utilized for spectral characterization of the object across selected operational states. Next, a predefined signal of a fluctuating frequency was generated to evaluate the self-tuning ability of the proposed control system.

### 4.3 Data acquisition

The structural response of the frame is acquired using laser sensors divided into two groups. The first group acquires data characterizing the kinematic response in predefined nodes, which serves as input for the controller. The second group monitors the quality of the control process.

The first set of sensors comprises six distance laser sensors (Baumer models 20U2460 and 20U2441), configured to measure displacements with a  $10~\mu m$  resolution within a 20~mm range. The measuring points are positioned at locations corresponding to all nodes established for numerical analysis. At each node, measurements are taken at two spots to gather displacements along the OX axis, as well as ongoing rotation in the OXY plane. For each node, the state vector includes: displacement along the OX axis, velocity along the OX axis, angle in the OXY plane, and angular velocity in the OXY plane. Data is acquired periodically into sets of 2 s duration at a 1 kS/s rate and used as input for the RL tuning module.

The second set of sensors consists of three distance laser sensors (Baumer model 20I6460; 20 mm range,  $10 \mu m$  resolution) that measure the displacement of the semi-active joints along the OX direction. The acquired data is used for evaluation of the control process performance.

## 4.4 Control application

Each semi-active joint pair can be used to modify the local stiffness of the frame. The control system tunes the structure's vibrational response by recognizing the current operating conditions and adjusting the settings to minimize the internal energy of the system. Activating or deactivating the joints affects the spectral response of the structure. Simultaneously, the state of the joints influences the internal damping across the frame.

The application for experimental testing executes the following algorithm during the control procedure: 1. Initialization of the system; 2. Calibration and configuration of the laser sensors; 3. Acquisition of a 2 s data sequence; 4. Data processing and conditioning; 5. Determination and visualization of the quality factor; 6. Formulation of the state vector; 7. Execution of the tuning procedure; 8. Update of the control parameters; 9. Introduction of a predefined delay; 10. Return to point 3. or exit.

### 5 CHARACTERIZATION OF STRUCTURAL DYNAMICS

In the numerical analysis, the structure is modeled as a 1D Timoshenko beam, with shear effects explicitly considered. The structure exhibits also semi-active functionality that intro-

duces a non-linear behavior into the system. To ensure the predictability of the experimental procedure, precise characterization of the experimental object is necessary. To achieve this, a spectral analysis of the frame was conducted for the following operational states:

- 1. Pairs 1+2+3 activated;
- 2. Pair 1 deactivated, Pairs 2+3 activated;
- 3. Pairs 1+2 deactivated, Pair 3 activated;
- 4. Pairs 1+2+3 deactivated.

Activation of a semi-active module is interpreted as the state with the ability to transfer bending moments. The investigated set of operational states reveals significant differences in the structural dynamics. These results are necessary for an adequate assessment of the internal energy in the frequency domain.

### 5.1 Results

The results of the spectral characterization are depicted in Figure 4 as Power Spectral Density (PSD) plots. The plots illustrate the influence of joint activation on the structural response of the frame. The experiment has covered the four operational states described above. Consecutive deactivation of the semi-active pairs decreased the fundamental eigenfrequency. A significant shift is observed when the first pair is deactivated: the frequency is drops from 9.9 Hz to 8.22 Hz, which indicates that the 1st pair of joints has the most substantial impact on the structural dynamics. This can be explained by its proximity to the support, where bending moments are the highest in comparison to the locations of the other pairs. Further changes in operational state (deactivating subsequent pairs) resulted in further decreases in the eigenfrequency. Deactivation of both the 1st and 2nd pairs reduced it to 8.08 Hz, while switching all nodes to the low-transfer mode resulted in a 7.97 Hz eigenfrequency. This sequence of eigenfrequency reductions is associated with the corresponding decrease in the bending stiffness of the frame.

Moreover, the examined operational configurations affect the structural damping exhibited by the frame. Similar to stiffness, the damping increases monotonically in the successive operational states. This increase may be the consequence of residual friction present in the semiactive joints in their deactivated state.

The characteristics shown in Figure 4 define the operational range available on the demonstration frame. They reveal that the structural dynamic characteristics can be effectively modified and emphasize the potential for optimal tuning in response to varying excitation.

### 6 ASSESSMENT OF THE RL CONTROL APPROACH

The developed RL control approach was verified in a series of exemplary trials. To confirm repeatability, the series consisted of 5 samples. The primary assumption for these trials was to subject the frame to an unknown excitation of a fluctuating character. The objective of the tuning algorithm was to adapt the semi-active components of the frame and minimize the amplitude of the vibrational response.

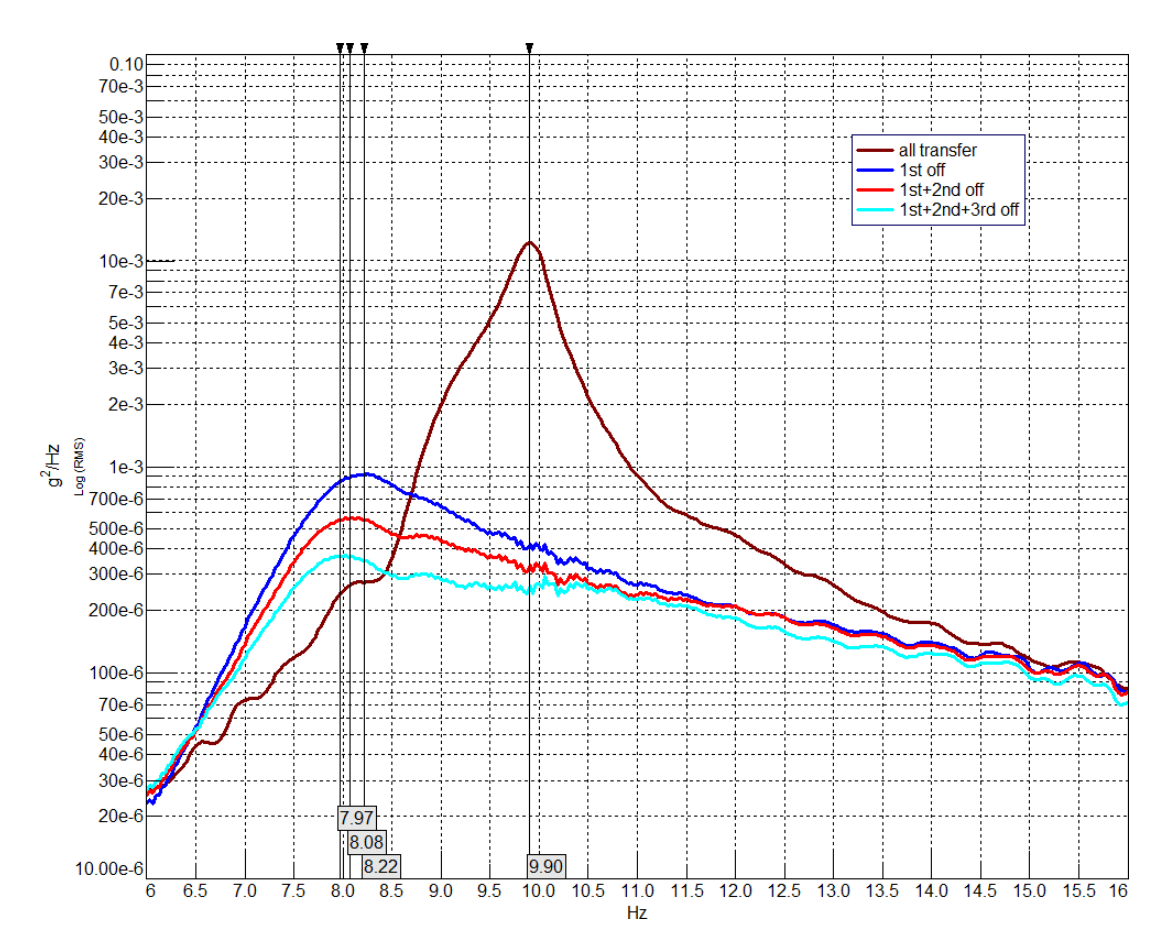


Figure 4: Spectral analysis (PSD functions)

The test demonstrates the self-tuning ability of the system for a stepwise switch of the excitation frequency from 10.5 Hz to 8.3 Hz. Initially, all semi-active joints were deactivated, which corresponds to a suboptimal state. Therefore, the initial response of the frame is characterized by an increased amplitude. Figure 5 depicts the time history of the system operation on four plots. The first plot depicts the excitation frequency as a step function, switching from 10.5 Hz to the target value of 8.3 Hz. The second plot illustrates the time evolution of control parameters related to the three semi-active pairs. It can be observed that the algorithm starts to adjust their values already one iteration after the change in excitation occurs. Since the semi-active pairs provide a bivalent operation while the control parameters are continuous in the range [0,1], a discrimination threshold of 0.7 is applied. The third plot shows the actuator states in time, where a value of 0 indicates low transfer of bending moments (deactivation), and a value of 1 denotes full transfer (activation). The fourth plot presents the RMS of vibration measured in three points of the frame. The RMS serves in this study as an analogue of structural energy, and it is used as a performance measure for quantification of control quality.

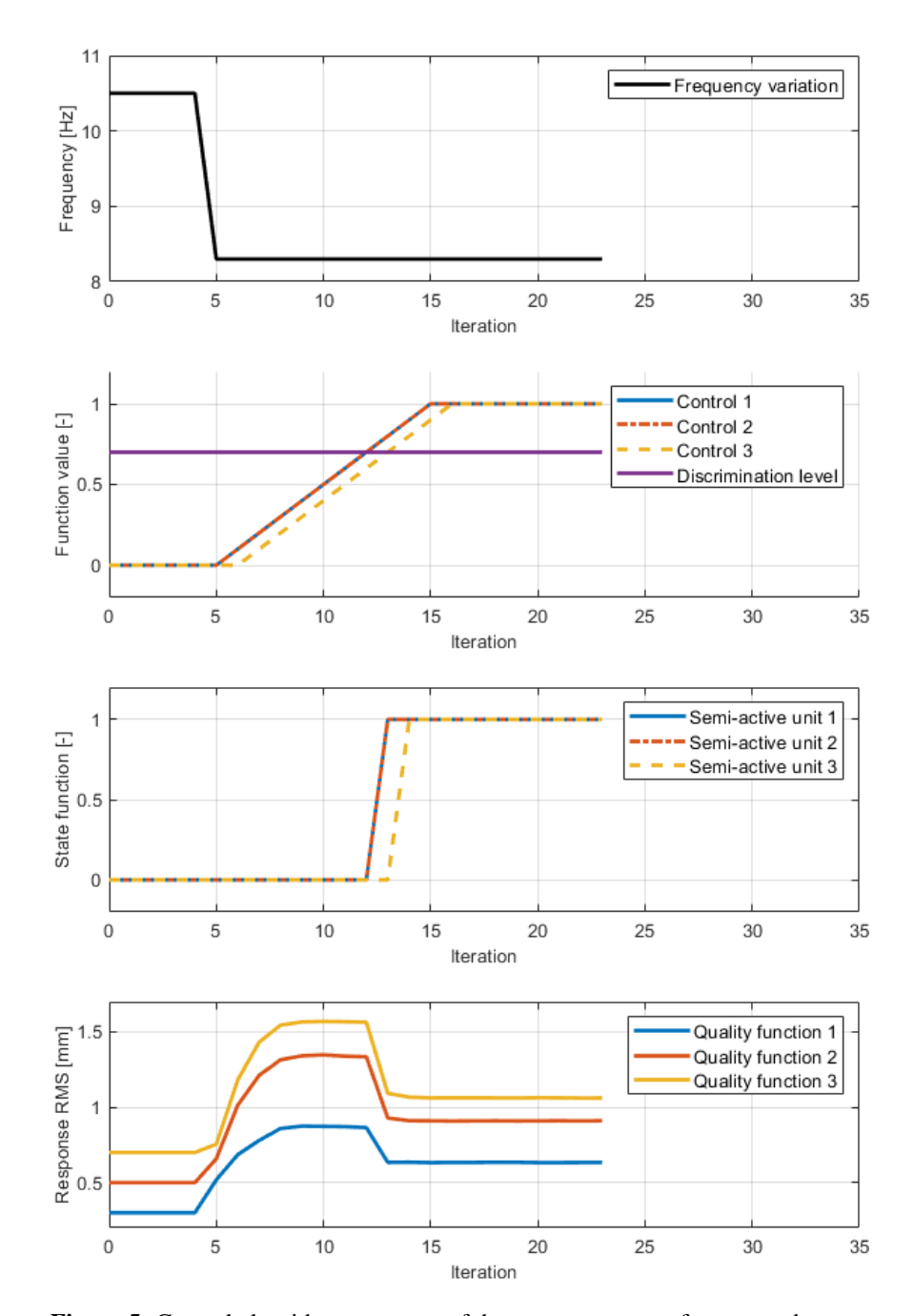


Figure 5: Control algorithm: response of the system to a step frequency decrease

As seen in Figure 5, the stepwise change in excitation frequency triggers an instant reaction of the algorithm and adjustments to the control parameters. The discrimination threshold is crossed at the 12th and 13th iterations, which results in changes of the actuator states. Semi-active unit No. 3 switches its state in the 13th iteration, and a gradual reduction of RMS values can be observed.

#### 7 CONCLUSIONS

This contribution presented preliminary results on vibration control in a frame structure equipped with semi-active members using a reinforcement learning approach. The study confirms the intended effective operation of the system. The algorithm has a potential for tuning the structural response under alternating external excitations and efficiently minimizing the amplitude of the vibration response.

### **ACKNOWLEDGEMENTS**

The authors gratefully acknowledge the support of the National Science Centre, Poland, granted under the grant agreement 2020/39/B/ST8/02615. For the purpose of Open Access, the authors have applied a CC-BY public copyright licence to any Author Accepted Manuscript (AAM) version arising from this submission.

#### REFERENCES

- [1] B. Basu, O. S. Bursi, F. Casciati, S. Casciati, A. E. Del Grosso, M. Domaneschi, L. Faravelli, J. Holnicki-Szulc, H. Irschik, M. Krommer, M. Lepidi, A. Martelli, B. Ozturk, F. Pozo, G. Pujol, Z. Rakicevic, and J. Rodellar, "A European Association for the Control of Structures joint perspective. Recent studies in civil structural control across Europe," *Structural Control and Health Monitoring*, vol. 21, no. 12, pp. 1414–1436, 2014.
- [2] S. Korkmaz, "A review of active structural control: challenges for engineering informatics," *Computers & Structures*, vol. 89, no. 23-24, pp. 2113–2132, 2011.
- [3] S. Hurlebaus and L. Gaul, "Smart structure dynamics," *Mechanical systems and signal processing*, vol. 20, no. 2, pp. 255–281, 2006.
- [4] M. Ostrowski, B. Błachowski, B. Popławski, D. Pisarski, G. Mikułowski, and Ł. Jankowski, "Semi-active modal control of structures with lockable joints: general methodology and applications," *Structural Control and Health Monitoring*, vol. 28, no. 5, p. e2710, 2021.
- [5] G. Mikułowski, B. Popławski, and Ł. Jankowski, "Semi-active vibration control based on switchable transfer of bending moments: Study and experimental validation of control performance," *Smart Materials and Structures*, vol. 30, no. 4, p. 045005, 2021.
- [6] H. Kurino, J. Tagami, K. Shimizu, and T. Kobori, "Switching oil damper with built-in controller for structural control," *Journal of Structural Engineering*, vol. 129, no. 7, pp. 895–904, 2003.
- [7] D. Silver, T. Hubert, J. Schrittwieser, I. Antonoglou, M. Lai, A. Guez, M. Lanctot, L. Sifre, D. Kumaran, T. Graepel, T. Lillicrap, K. Simonyan, and D. Hassabis, "A general reinforcement learning algorithm that masters chess, shogi, and go through self-play," *Science*, vol. 362, no. 6419, p. 1140–1144, 2018.

- [8] G. Reddy, A. Celani, T. Sejnowski, and M. Vergassola, "Learning to soar in turbulent environments," *Proceedings of the National Academy of Sciences*, vol. 113, no. 33, pp. E4877–E4884, 2016.
- [9] Y. Jiao, F. Ling, S. Heydari, N. Heess, J. Merel, and E. Kanso, "Learning to swim in potential flow," *Physical Review Fluids*, vol. 6, p. 050505, 2021.
- [10] H. Shi, Y. Zhou, X. Wang, S. Fu, S. Gong, and B. Ran, "A deep reinforcement learning-based distributed connected automated vehicle control under communication failure," *Computer-Aided Civil and Infrastructure Engineering*, vol. 37(15), pp. 2033–2051, 2022.
- [11] Y.-A. Zhang and S. Zhu, "Novel model-free optimal active vibration control strategy based on deep reinforcement learning," *Structural Control and Health Monitoring*, vol. 2023, p. 6770137, 2023.
- [12] Z. Qiu, G. Chen, and X. Zhang, "Reinforcement learning vibration control for a flexible hinged plate," *Aerospace Science and Technology*, vol. 118, p. 107056, 2021.
- [13] A. Khalatbarisoltani, M. Soleymani, and M. Khodadadi, "Online control of an active seismic system via reinforcement learning," *Structural Control and Health Monitoring*, vol. 26, no. 3, p. e2298, 2019.
- [14] C. Dengler and B. Lohmann, "Actor-critic reinforcement learning for the feedback control of a swinging chain," *IFAC Papers*, vol. 51, p. 378–383, 2018.
- [15] B. Adam and I. Smith, "Reinforcement learning for structural control," *Journal of Computing in Civil Engineering*, vol. 22, no. 1, pp. 133–139, 2008.
- [16] D. Pisarski and Ł. Jankowski, "Reinforcement learning-based control to suppress the transient vibration of semi-active structures subjected to unknown harmonic excitation," *Computer-Aided Civil and Infrastructure Engineering*, vol. 38(12), pp. 1605–1621, 2023.
- [17] A. Jedlińska, D. Pisarski, G. Mikułowski, B. Błachowski, and Ł. Jankowski, "Semi-active structural control using viscous dampers and reinforcement learning," in *Proceedings of the 10th ECCOMAS Thematic Conference on Smart Structures and Materials, SMART 2023*, Patras, Greece, July 2023, pp. 589–596.
- [18] A. Jedlińska, D. Pisarski, G. Mikułowski, B. Błachowski, and Ł. Jankowski, "Semi-active control of a shear building based on reinforcement learning: Robustness to measurement noise and model error," in *Proceedings of the 18th Conference on Computer Science and Intelligence Systems, FedCSIS 2023*, Warsaw, Poland, September 2023, pp. 1001–1004.
- [19] A. Jedlińska, D. Pisarski, G. Mikułowski, B. Błachowski, and Ł. Jankowski, "Damage-aware structural control based on reinforcement learning," in *Proceedings of the 11th European Workshop on Structural Health Monitoring, EWSHM 2024*, Potsdam, Germany, June 2024.